Field-driven transitions in the dipolar pyrochlore antiferromagnet $Gd_2Ti_2O_7$

Olivier Cépas[1] and B. Sriram Shastry[1,2]
[1]*Department of Physics, Indian Institute of Science, Bangalore 560012, India*
[2]*Department of Physics, University of California, Santa Cruz, California 95064, USA*
(Received 18 June 2003; revised manuscript received 3 November 2003; published 6 May 2004)

We present a mean-field theory for magnetic-field-driven transitions in dipolar coupled gadolinium titanate $Gd_2Ti_2O_7$ pyrochlore system. Low-temperature neutron scattering yields a phase that can be regarded as a eight sublattice antiferromagnet, in which long-ranged ordered moments and fluctuating moments coexist. Our theory gives parameter regions where such a phase is realized, and predicts several other phases, with transitions amongst them driven by magnetic field as well as temperature. We find several instances of *local* disorder parameters describing the transitions.

DOI: 10.1103/PhysRevB.69.184402 PACS number(s): 75.10.Hk

I. INTRODUCTION

The pyrochlore $S=7/2$ Heisenberg spin system $Gd_2Ti_2O_7$ is currently very popular. In addition to magnetic ordering at 1 K (Ref. 1) which is not expected for a Heisenberg pyrochlore system,[2] it displays magnetic-field-driven phase transitions that are intriguing, and have been ascribed to the competition between dipole-dipole (d-d) interactions and the Zeeman energy on frustrated *and* undistorted cubic systems.[3] The exchange energy has been argued to be relatively small, due to the compact *f* shell of Gd, but nevertheless plays an important role in lifting the degeneracy between various possibilities, as we show in this work.

Earlier examples of similarly low-energy scales are known, but on the diamond lattice[4] and the gadolinium gallium garnet,[5] thus lacking the complexity of the pyrochlores. Theoretical interest in d-d coupled systems is quite old,[6] focusing on its long-ranged nature.

$Gd_2Ti_2O_7$ is intriguing, first by the magnetic order it displays at low temperatures and zero magnetic field, as observed by neutron scattering.[7] The magnetic order has been assigned a propagation vector $\mathbf{q}=\{\pi,\pi,\pi\}\equiv\boldsymbol{\pi}$ at 50 mK, and the interstitial moments[8] are zero on average, thus showing a partially ordered state despite the very low temperature.[7] This structure is consistent with the correlations observed at higher temperatures in electron spin resonance (ESR).[9] This turns out to be in direct conflict with previous theoretical works that assumed a nearest-neighbor Heisenberg system with d-d interactions. The expansion of the free energy to quadratic order in the order parameter near the ordering temperature T_N tells us that all the states with a propagation vector along the (111) direction become unstable simultaneously.[1] Such a degeneracy is in fact not quite exact; refined numerics and analytical work show that the $\mathbf{q}=\boldsymbol{\pi}$ state is very slightly preferred.[10] Nevertheless, below T_N the fourth-order term in the free energy expansion becomes important and favors a $q=0$ state,[11] which has been confirmed by a real-space mean-field theory employing a four-sublattice decomposition of the pyrochlore lattice.[3] From these works, however, it is not clear as to how this $\mathbf{q}=\boldsymbol{\pi}$ state can be realistically and *robustly* realized. We find that this requires going beyond the nearest-neighbor exchange model studied previously.

The second particularly interesting feature of gadolinium titanate is the presence of magnetic-field-driven phase transitions.[3] For cubic systems one expects exotic phases connected by continuous transitions, as compared to well-studied first-order spin-flop-type transition on uniaxially distorted systems, such as MnF_2. Although the four-sublattice mean-field theory is in conflict with the neutron-scattering results, it gives such field-driven transitions with critical fields in rough agreement with those observed on a powder sample.[3]

The aim of the present paper is to show that a model that includes exchange energies beyond the nearest neighbors not only explains the magnetic structure observed by neutron scattering at low temperatures but also exhibits magnetic-field-driven transitions whose features can be checked by further experimentation. We present the results of the expansion of the free energy near T_N together with a low-temperature mean-field theory using ''hard spins'' (that describes the fixed length constraint well) that is, hence, valid at all temperatures, although limited by the sublattice structure imposed at the outset. The earlier analysis[3] imposed a four-sublattice order, here we go to the next level of description, namely a eight-sublattice order, in order to accommodate the $\mathbf{q}=\boldsymbol{\pi}$ state. This allows us to find other stable phases.

We begin by summarizing the results of the hard-spin mean-field theory. The 8-sublattice system consists of two tetrahedra (see Fig. 1), the second one being obtained by a translation of the first one along the primitive vector (110). There are four other such equivalent directions that would give equivalent results, in particular with regards to the propagation vector $\boldsymbol{\pi}$. Without loss of generality, we consider only one of them in the following, namely (111).

II. ZERO-MAGNETIC-FIELD PHASES

The pyrochlore lattice sustains various phases. We have alluded to the $\mathbf{q}=\mathbf{0}$ phase previously, which we denote as *A* in the present work. It has a sixfold degeneracy according to

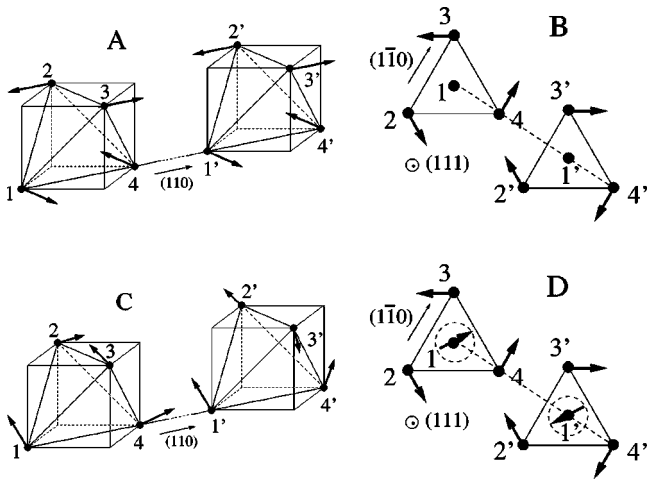

FIG. 1. On the left, the eight sublattices used in the mean-field calculation are shown. The *A* state ($q=0$) is shown (sixfold degenerate). On the right, the spins of the *B* state (degeneracy 2) belong to the Kagomé planes; the sublattices 1 and $1'$ have no magnetic moment in average. The *D* state is identical to *B* except that the magnetizations of the sublattices 1 and $1'$ are finite and opposite from one Kagomé plane to the next (continuous degeneracy). *C* does not have any simple description (see text).

the three planes of the cubic structure and the time-reversal symmetry.[11,3] In addition, there are three other phases that we call *B*, *C*, and *D*, that break translation invariance.

At finite temperatures, and for different (exchange) parameters, we find a distinct phase *B*, which can be described as a $\mathbf{q}=\boldsymbol{\pi}$ state. In this phase, the interstitial sites have, on average, no magnetic moment. The spins of the Kagomé planes, on the other hand, are ordered in a 120 deg structure; each of them being parallel to the opposite edge in order to minimize the d-d interactions. This is the phase that has been found experimentally in $Gd_2Ti_2O_7$.

There is also a phase that we call *C* which does not have a simple description: the interstitial spins $(1-1')$ are parallel to each other and the other spins break translational symmetry and are not coplanar. There are 12 such degenerate states. It seems plausible that the *C*-type phases are in reality the ''projection'' onto the eight-sublattice of incommensurate states.

In addition to these phases which all have a finite degeneracy, we have found a phase *D*, which is particularly interesting in that it has a continuous degeneracy. We emphasize here that we actually start from a strongly frustrated system, whose huge degeneracy is lifted by the d-d interactions. It is therefore surprising to obtain a continuously degenerate ground state in a wide range of parameters when further neighbor interactions are switched on. In the *D* phase, the spins of the Kagomé planes are identical to those of the *B* phase. The interstitial moments, however, are finite. They may point in any direction in a plane parallel to the Kagomé planes, giving a large degeneracy, and they are antiparallel to each other from plane to plane. This is actually the zero-temperature analog of the *B* phase, but occurs at low temperatures.

To find those phases, we have considered the Hamiltonian

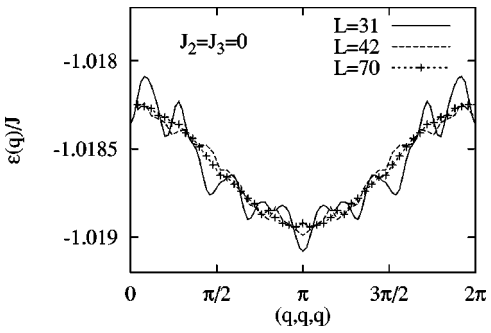

FIG. 2. Quasidegeneracy of the lowest eigenvalue as function of $\mathbf{q}$ along (111) for $J_2=J_3=0$ (see the vertical scale). When L [the number of neighbors in the (100) direction included in the dipolar sums] is increased, the curves converge to a smooth curve which minimum is at, or very close to, $\mathbf{q}=\boldsymbol{\pi}$.

defined on the pyrochlore lattice

$$\mathcal{H}=\frac{1}{2}\sum_{ij} J_{ij}\mathbf{S}_i\cdot\mathbf{S}_j-g\mu_B\sum_i \mathbf{S}_i\cdot\mathbf{H}+(g\mu_B)^2 \times\sum_{ij}\left(\frac{\mathbf{S}_i\cdot\mathbf{S}_j}{r_{ij}^3}-3\frac{(\mathbf{r}_{ij}\cdot\mathbf{S}_i)(\mathbf{r}_{ij}\cdot\mathbf{S}_j)}{r_{ij}^5}\right), \quad (1)$$

where $\mathbf{S}_i$ is a quantum spin operator for spins $S=7/2$ on site i. J_{ij} is the Heisenberg exchange between the neighbors: we are in fact considering the first neighbors at a distance $a_0=3.59$ Å (J), the second (J_2, distance $\sqrt{3}a_0$), and third neighbors (J_3, distance $2a_0$). We note that there are in fact two types of third-neighbor exchanges according to the crystal structure. The difference of them being another small parameter, we will neglect it in the following. Let us first describe the ''k-space'' mean-field theory. We have studied the stability of the paramagnetic state towards a state with a modulation vector k, extending Ref. 1 to include J_2 and J_3. By expanding the free energy near T_N, we get a 12×12 matrix, its lowest eigenvalue determines T_N and the corresponding eigenvector describes the k modulation of the state. We find that the degeneracy along (111) (Refs. 1,11) for $J_2=J_3=0$ is actually weakly lifted when the dipolar sums include a larger number of neighbors compared with previous works, as previously noticed.[10] The selected mode is at, or very close to, $\mathbf{q}=\boldsymbol{\pi}$ (see Fig. 2). New numerical work using the Ewald summation technique has indeed clearly shown that this mode is selected.[12] Nevertheless, in order to robustly lift what remains a quasidegeneracy, it is important to include J_2 and J_3. As soon as $J_2<0$, $\mathbf{q}=\boldsymbol{\pi}$ is robustly selected. The corresponding eigenvector tells us that it corresponds to the *B* state. There are two other regions of the phase diagram where the *A* phase and an incommensurate phase are preferred. The phase diagram of the first instability is given in dashed lines in Fig. 3. Since the above approach can only give the first instability that is encountered on cooling, i.e., at T_N, nothing is known about the lower-temperature behavior of the system. We therefore proceed to a real-space mean-field theory following Ref. 3, but enlarging the unit cell to eight sublattices, as already specified.

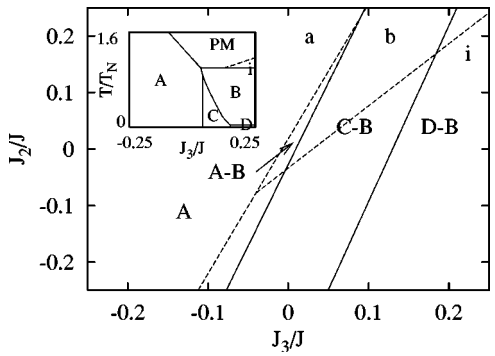

FIG. 3. Phase diagrams showing the first unstable modes of the paramagnetic phase at T_N (dashed line, small letters, "*i*" for incommensurate) and from the eight-sublattice mean-field theory (solid line, capital letters). In the inset, the phase diagram as a function of temperature is shown for $J_2=0.1J$. T_N is the temperature to enter the *B* phase at intermediate J_3. $J=0.4$ K.

Within the mean-field theory, the magnetizations of the sublattices are given by $\langle \mathbf{S}_a \rangle = S\hat{\mathbf{h}}_a \mathcal{B}_S(\beta h_a S)$ with the definitions of the local fields, $h_a^\alpha \equiv g\mu_B H^\alpha - \Sigma_{b\beta} J_{ab}^{\alpha\beta} \langle S_b^\beta \rangle$, where $\mathcal{B}_S$ is the Brillouin function and β is the inverse temperature. $J_{ab}^{\alpha\beta}$ couples the sublattices *a* and *b*, running from 1 to 8. A straightforward way of solving the problem consists of iterating numerically these self-consistent equations, starting from many random configurations and selecting the set of states with the lowest free energy. This leads to the phase diagram given in Fig. 3 (solid lines). The phases *A*, *C*, and *D* described above are found at zero temperature in quite a narrow and physically reachable region of parameters. However, there is no sign at zero temperature of the *B* phase found in the mode analysis.

In Fig. 3, we give the labels for the sequence of phases on increasing *T* prior to reaching the paramagnetic phase. Details of the transition temperatures for the eight-sublattice problem are given in the inset of Fig. 3 for a given $J_2=0.1J$ (solid lines). For $J_2=J_3=0$, as another example, the *A* phase is definitely chosen below T_N, in agreement with Refs. 11 and 3. The transition to the *B* state at T_N, as suggested in the mode analysis given above (Fig. 2), is in fact immediately followed by a transition to the *A* phase when the temperature is decreased (so that on the scale of Fig. 4, the *B* phase is indistinguishable at the PM-*A* transition). To robustly select the *B* phase in a wide range of temperatures (as experimentally observed), it is necessary to include other interactions, the simplest assumption being the next-nearest Heisenberg couplings. Indeed, when J_3 is increased or J_2 decreased, the region where we have the *A*-*B* succession of phases widens (see inset of Fig. 3), before the onset of the other phases. For these other phases, the *C*-*B* transition line appears to be first order, whereas *D*-*B* is second order.

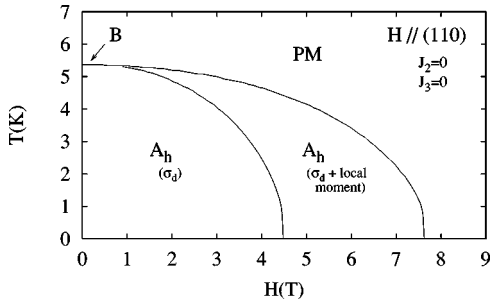

FIG. 4. Phase diagram (H,T) for a magnetic field parallel to (110), showing the broken symmetries (in brackets). A_h represents the *A* phase under field. The *B* phase occurs in a very narrow region near T_N at $H=0$ (see text).

We can now compare in more detail these results with those of the *k*-space mean-field theory, i.e., the stability analysis of the paramagnetic state. For large portions of the phase diagram (where the last capital letter coincides with the small letter), the two approaches give the same result. There is, however, a region of parameters (e.g., large J_3) where the first unstable mode is incommensurate, while for the same parameters we find a transition from the paramagnetic state to the *B* state in the eight-sublattice calculation. The eight-sublattice calculation cannot capture the first transition to the incommensurate state because of the sublattice decomposition. On the other hand, such a calculation respects the fixed length constraint of the spins at low temperatures. Within this point of view, two scenarios may take place when the temperature is lowered. In both of them there is first a transition from the paramagnetic state to the incommensurate state. Then the incommensurate state may exist down to zero temperature and the occurrence of the *B* state is a pure artifact of the sublattice calculation. Alternatively, the *B* state *is* stabilized at low temperature. In this case there must be a phase transition between the incommensurate state and the *B* state when the temperature is lowered. In order to rule out one scenario, one would need to study the stability of the phases at low temperature bypassing the limitations of the sublattice decomposition.

III. MAGNETIC-FIELD-DRIVEN TRANSITIONS

A magnetic field is an interesting probe of these phases. We highlight here the main results on all four phases since we believe that the *A*, *C*, and *D* phases might be useful for other materials. The *A* phase gives rise to multiple phase transitions, as previously reported for $T=0$.[3] We note, however, several new elements arising from the effect of finite temperatures. In Fig. 4, we give the example of the complete phase diagram when the field is along (110). For small enough fields, a raise in temperature drives the system through two phase transitions, a result which also holds for the fields along the other crystallographic directions, (100) and (111), with, in the latter case, a first transition which is weakly first order.

Although the two successive phases A_h for a field along (110) are separated by a transition line (see Fig. 4), they cannot be distinguished by a different *geometrical* broken symmetry. They basically bear the same σ_d broken symmetry, but none of the other geometrical symmetries is broken in either phase. The effect of thermal fluctuations turns out to be crucial in distinguishing them. Indeed, at any finite temperatures, this transition is associated with the occurrence of a *disorder* parameter—a quantity which is zero in the or-

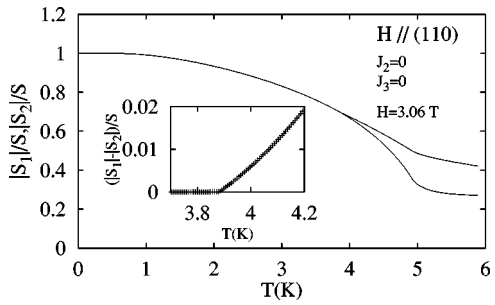

FIG. 5. Local magnetic moments averaged by the thermal fluctuations as function of temperature. Above the first transition, we see a difference in the moments of the two sublattices that are inequivalent because of the field. The difference is a *disorder* parameter for one transition, with a critical exponent numerically close to 4/3.

dered phase and nonzero in the disordered phase, which we now describe. When we look at the value of the magnetic moment (smaller than S as soon as $T>0$), it appears that in the ordered phase all the magnetic moments of the four sublattices are the same, while they are different above the first transition (Fig. 5). We can thus define a *disorder parameter* by the difference of two of these moments (inset of Fig. 5). Moreover, we have found that the disorder parameter has a critical exponent $\sim 4/3$. This is in contrast with the other linear order parameters which follow the usual 1/2 exponent of the Landau theory. One remarkable feature to note is that our disorder parameters are *local*. This is quite unlike the familiar disorder parameters that arise in theories with duality that lead naturally to highly nonlocal disorder parameters, such as are known for the 2-d Ising model.

We note that these transitions are quite different from the classical spin-flop transitions of the uniaxial antiferromagnets. In addition to those unconventional mean-field exponents, the response of the spins themselves is worth mentioning. When a field along (100) is increased, for instance, the spins 1 and 2 of the A phase (or 3 and 4) which are perpendicular to each other at zero field, remain exactly perpendicular while the sum of both spins twist towards the field. This is not obvious and in particular cannot be understood by considering partial couples, since it is a real four-sublattice-coupled system.

The effect of a magnetic field on the B phase is to induce back a net magnetic moment on the previously zero-moment interstitial sites. At higher fields along the (111) or (100) directions, there is a unique transition to the paramagnetic phase with a merging of the two degenerate states (Fig. 6). For the $(1\bar{1}0)$ direction, however, there is a reentrance of a less symmetric phase when the magnetic field is increased. This phase is fourfold degenerate and breaks the mirror plane symmetry. At larger fields the twofold degenerate state is recovered before reaching the transition to the paramagnetic state. In total, there are three main distinct transitions when the field is increased from zero because the critical field of the paramagnetic transition depends very weakly upon the direction of the field.

Regarding the C or D phases, we have to describe what happens to the interstitial moments before the system enters

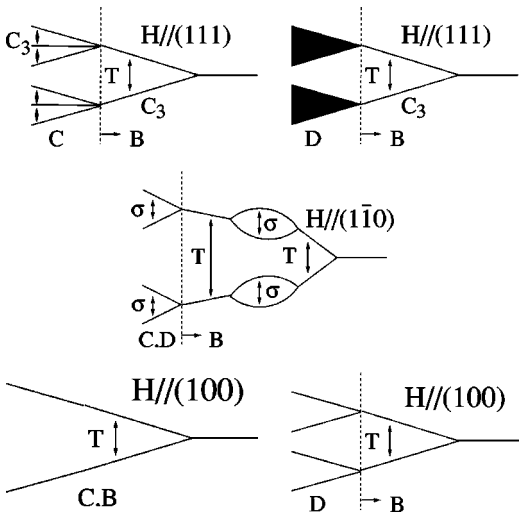

FIG. 6. Evolution of the degeneracies as a function of an external magnetic field along the main crystallographic directions. The broken symmetries and the symmetries that connect the distinct states are also given (T is the translation operation, σ a mirror plane, and C_3 a threefold rotation). Dark shading indicates continuous degeneracy of the state.

the B phase and undergoes the transitions described above. For the D phase, the continuous degeneracy is preserved with a field along (111), until the B phase is reached. For the other directions, the degeneracy is lifted at an infinitesimal field by a spin-flop transition for the interstitial moments. For the C phase, the situation is very similar (see Fig. 6).

IV. COMPARISON WITH EXPERIMENTS

We now compare our theoretical calculations with experimental results on $Gd_2Ti_2O_7$. The success of this approach is to predict the existence of the $\mathbf{q}=\boldsymbol{\pi}$ phase in a wide range of temperatures and parameters. Although it is not the ground state of the problem (since only A, C, and D phases are obtained at zero temperature), the B phase may be stabilized at very low temperatures, as observed experimentally. This is obtained with parameters J_2 and J_3 typically of the order of $0.1J$ which are physically reasonable. Next-nearest-neighbor Heisenberg interactions may indeed take place in these materials, especially if we think of an exchange mechanism in terms of a magnetic exchange between the f electrons and the more extended d electrons which may carry the spin polarization at distances larger than the nearest neighbors.[13] We give the phase diagram for typical parameters in Fig. 7, which reproduces the number of field-driven transitions observed experimentally. We have two free parameters, J_2/J and J_3/J, chosen typically as -0.125 and 0.1, and J is then fit to the measured high-temperature susceptibility. The values of the critical fields measured at low temperatures ($3T$, $6T$, and $7T$) are then well reproduced. Spin susceptibilities are given in the inset of Fig. 7. Note that the powder-averaging susceptibility is almost featureless and does not account for the complexity of the transitions.

Also interesting are the ESR results in the paramagnetic phase.[9] In addition to anisotropic properties, the ESR signal

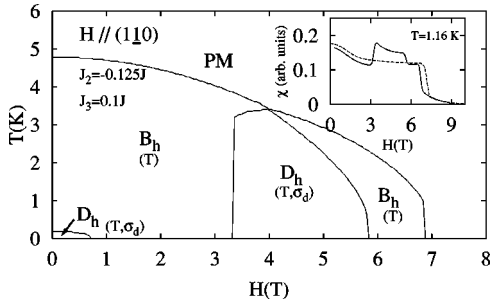

FIG. 7. Phase diagram (H,T) for a magnetic field parallel to $(1\bar{1}0)$, showing the various phases and the broken symmetries (in brackets). D_h represents the D phase under field. Insert: Spin susceptibility for $H\|(1\bar{1}0)$, convoluted with a Gaussian function (solid line) and powder-averaged susceptibility (dashed line).

shows two lines, revealing the existence of two inequivalent sites, though since no structural distortions have been reported, the four sites of the unit-cell should be equivalent. We note, for example, that distortions that would strengthen the magnetic interactions in the Kagomé planes would naturally help to select the B phase. Even in the absence of distortions, the applied magnetic field (which is necessary to perform the ESR studies) breaks some symmetries of the lattice. In this respect, and although the sublattices are equivalent at zero magnetic field, we have found different averaged magnetic moments on two different sites under magnetic field. Therefore, we naturally expect two lines to appear in the high-temperature ESR spectrum. Note in particular that the difference of magnetic moments is precisely what we found to be a disorder parameter in one transition at low temperature (Fig. 5). In any case, it is an interesting example where ESR would not probe the properties of the zero-field state. This is of course expected from symmetry considerations, but we have found here a simple example of a system where it does occur.

The phase diagram as a function of the model parameters (Fig. 3) may be relevant to other compounds as well. The chemical replacement (of Ti by Sn, for instance), or an external pressure could well drive the system into either of the other phases because of the modifications in the magnetic exchange paths, and hence the relative strengths of J, J_2, and J_3. A different behavior has indeed been found experimentally in $Gd_2Sn_2O_7$ at low temperatures.[14] Although this system orders at a similar temperature, the moments were suggested to be perpendicular to the local (111) directions on the basis of Mössbauer measurements.[14] Such a magnetic ordering, if confirmed by neutron scattering, would be more compatible with the A phase.

V. CONCLUSION

In summary, we have found several phases and phase transitions in the dipolar pyrochlore lattice by taking into account the magnetic exchange beyond the nearest-neighbor Heisenberg coupling. One of them is precisely the B phase of $Gd_2Ti_2O_7$ seen in neutron scattering.[7] We find that it is not the ground state, but a finite temperature state. We obtain, as ground states, the A, C, or the degenerate D phase. When a magnetic field is applied, we find that the B phase undergoes three transitions, as appeared in specific-heat measurements. We have predicted the corresponding magnetic structures and the broken-symmetry phases that could be checked by neutron-diffraction experiments. Sound velocity and absorption studies, as well as calorimetric studies with aligned crystals in magnetic fields, should shed light on the nature of the phases predicted here.

ACKNOWLEDGMENTS

We thank Art Ramirez and David Huse for stimulating discussions and for constructive suggestions, and R. Karan for numerical help. We acknowledge support from an Indo-French grant, Grant No. IFCPAR/2404.1.

[1] N.P. Raju, M. Dion, M.J.P. Gingras, T.E. Mason, and J.E. Greedan, Phys. Rev. B **59**, 14489 (1999).
[2] R. Moessner and J.T. Chalker, Phys. Rev. Lett. **80**, 2929 (1998); Phys. Rev. B **58**, 12049 (1998).
[3] A.P. Ramirez, B.S. Shastry, A. Hayashi, J. Krajewski, D. Huse, and R.J. Cava, Phys. Rev. Lett. **89**, 067202 (2002).
[4] S.J. White, M.R. Roser, Jingchun Xu, J.T. van der Noordaa, and L.R. Corruccini, Phys. Rev. Lett. **71**, 3553 (1991).
[5] P. Schiffer, A.P. Ramirez, D.A. Huse, and A.J. Valentino, Phys. Rev. Lett. **73**, 2500 (1994); O.A. Petrenko, C. Ritter, M. Yethiraj, and D. McK Paul, *ibid.* **80**, 4570 (1998); O.A. Petrenko and D.McK. Paul, Phys. Rev. B **63**, 024409 (2001).
[6] J.M. Luttinger and L.M. Tisza, Phys. Rev. **70**, 954 (1946).
[7] J.D.M. Champion, A.S. Wills, T. Fennell, S.T. Bramwell, J.S. Gardner, and M.A. Green, Phys. Rev. B **64**, 140407 (2001).
[8] The pyrochlore lattice can be regarded as a set of Kagomé planes connected by ''interstitial'' gadolinium sites that link the planes.
[9] A.K. Hassan, L.P. Lévy, C. Darie, and P. Strobel, Phys. Rev. B **67**, 214432 (2003).
[10] D. Huse (unpublished).
[11] S.E. Palmer and J.T. Chalker, Phys. Rev. B **62**, 488 (2000).
[12] M. Enjalran and M.J.P. Gingras, cond-mat/0307152 (unpublished).
[13] G. Bouzerar and P. Krüger (private communication).
[14] E. Bertin, J.A. Hodges, J.-P. Bouchaud, P. Bonville, J.-P. Sanchez, and P. Vuillet, Eur. Phys. J. B **27**, 347 (2002).